The electronic structure of $CuCl_2$ and $CuBr_2$ from anion photoelectron spectroscopy and *ab initio* calculations

Xue-Bin Wang and Lai-Sheng Wang
Department of Physics, Washington State University, 2710 University Drive, Richland, Washington 99352 and W. R. Wiley Environmental Molecular Science Laboratory, Pacific Northwest National Laboratory, P.O. Box 999, Richland, Washington 99352

Reuben Brown and Peter Schwerdtfeger
Department of Chemistry, University of Auckland, Private Bag 92019, Auckland, New Zealand

Detlef Schröder and Helmut Schwarz
Institut für Organische Chemie, Technische Universität Berlin, Straße des 17. Juni 135, D-10623 Berlin, Germany

(Received 17 November 2000; accepted 16 February 2001)

The electronic structures of CuX_2 (X=Cl and Br) have been investigated in the gas phase by means of anion photodetachment photoelectron spectroscopy and *ab initio* theory. The photoelectron spectra of CuX_2^- were recorded at two photon energies, 193 and 157 nm. Well-resolved and rich photodetachment features in the spectra provide unprecedented details for the low-lying electronic states of $CuCl_2$ and $CuBr_2$. The excitation energies for five low-lying electronic states of CuX_2 were determined, and they explain well the two previously observed optical absorption bands. The electron affinities for $CuCl_2$ and $CuBr_2$ were determined to be identical, 4.35 ± 0.05 eV within the experimental uncertainty. Both the anions and neutral CuX_2 species were calculated to be linear with only a slight bond length variation between the charged and neutral species. The calculated electron affinities and vertical excitation energies for the excited states agree well with the experimental values, yielding a definite assignment for the electronic states of $CuCl_2$ and $CuBr_2$.
 [DOI: 10.1063/1.1362289]

I. INTRODUCTION

Copper is a key cofactor in many biological oxidation–reduction reactions.[1] The Cu(I)/Cu(II) redox pair is one of the most common systems involved in a variety of electron-transfer enzymes. Characterization of the structure and spectroscopy of copper complexes at the active site in metalloproteins has been intensively pursued.[2–5] One of the ultimate goals is to understand the electronic structures of the copper complexes and their contributions to the biological functions. Here, we consider the gaseous species CuX_2^- and CuX_2 (X=Cl, Br) as simple models for the Cu(I)/Cu(II) redox pair. In terms of the d electron configuration, $CuCl_2$ is one of the simplest transition-metal dichlorides. In the ionic limit, the molecule is $Cl^-Cu^{2+}Cl^-$, where Cu^{2+} has d^9 configuration. While in the covalent limit, the Cu atom is promoted to the $3d^94s^2$ excited state, undergoes $4s-4p$ hybridization, and forms covalent bonds with the two Cl atoms. The ligand-field states are then derived from a $3d^9$ occupation of Cu^{2+} with a single hole in the $3d$ shell. Transitions between these states are referred to as $d-d$ excitations since they involve only changes in the orientation of the $3d$ hole. The charge transfer (CT) states are derived from a $3d^{10}$ occupation of Cu^+ and involve the transfer of one electron from the ligand to the metal.

The optical absorption spectrum of $CuCl_2$ exhibits two broad bands with maxima at $\sim$9 000 cm^{-1} (IR band) and 19 000 cm^{-1} (red band).[6,7] Several theoretical calculations have been carried out to interpret and assign the two optical bands.[8–11] A consensus has been reached that the ground state of $CuCl_2$ is $^2\Pi_g$ (Refs. 9–11) and not $^2\Sigma_g^+$ as predicted by simple ligand field calculations or as is the case for CuF_2.[6,7,12] However, there is no agreement in the assignment of the optical bands and the energetics of the low-lying electronic states among the calculations. There have been quite extensive high-resolution spectroscopic studies on $CuCl_2$ more recently. Rotationally resolved excitation spectra have been obtained both in a seeded molecular beam by recording the total fluorescence signal[13] and in a hot cell using laser-induced-fluorescence.[14–17] These studies[13] revealed that the ground state of $CuCl_2$ is $^2\Pi_{g(3/2)}$, and not $^2\Pi_{g(1/2)}$ as predicted theoretically,[9] and yielded detailed spectroscopic constants for the ground state. The interest in gaseous $CuCl_2$ has been stimulated recently by the observation of unexpected red and near-infrared bands in experiments intended to search for new chemical lasers.[18,19] It is now known that the near-infrared bands are due to the $CuCl_2$ emission at $\sim$9 000 cm^{-1},[20–22] but there is no agreement concerning the origin of the red band. Some works suggested that the red band was due to $CuCl_2$,[20,21,23] but others assigned it to other species,[22,24] such as excited chlorine oxides. It is surprising that there is not yet agreement on the energy levels among the low-lying states of a seemingly simple molecule as $CuCl_2$. This state of affair is most likely due to two reasons: (1) not many spectroscopic techniques can probe and resolve a manifold of low-lying electronic states, and (2) the correlation effects, which are very important in transition metals,

were not fully considered in the previous theoretical calculations.

We have developed an experimental technique to investigate solution-phase anionic species in the gas phase using photodetachment photoelectron spectroscopy (PES) and an electrospray ionization source coupled with ion-trap mass spectrometry.[25] As shown previously,[26–30] this technique is well suited to probe both multiply charged and singly charged metal complex anions, providing unprecedented details of molecular electronic structure information. PES of singly charged anions is a powerful tool in providing electronic and spectroscopic information about the underlying neutral species. The observed features represent transitions from the electronic ground state of the anion to the ground and excited states of the corresponding neutral molecule. Unlike optical absorption, which is subject to stringent selection rules, PES of an anion can access electronic states of the neutral molecules, which are optically ''dark.'' Here, we report a combined PES and *ab initio* study on CuX_2^- ($X=Cl, Br$) and the assignment for all the low-lying states of the corresponding neutral CuX_2 species. In addition, CuX_2^-/CuX_2 ($X=Cl, Br$) is the simplest molecular pair that contains the Cu(I)/Cu(II) redox couple. Therefore, photodetachment of gaseous CuX_2^- ($\rightarrow CuX_2+e^-$) is analogous to a redox reaction in solution beside the solvation effects. Hence, photodetachment of CuX_2^- will not only yield valuable electronic information for the CuX_2 molecules, but may also provide interesting information about solution redox reactions involving the Cu(I)/Cu(II) redox couple.

II. EXPERIMENTAL DETAILS

The experiment was carried out with an apparatus that includes a magnetic-bottle time-of-flight photoelectron analyzer and an electrospray ion source. Details of this apparatus have been reported recently,[25] and only a brief description of the experimental procedure is given here. To produce the desired anions, we used 10^{-3} molar solutions of tetraethylammonium tetrachloro and tetrabromo cuprate(II), $(NEt_4)_2CuCl_4$ and $(NEt_4)_2CuBr_4$, respectively, at pH$\sim$7 in a water/methanol (1:9 ratio) mixed solvent. The solutions were sprayed through a 0.01 mm diam syringe needle at ambient atmosphere and -2.2 kV high voltage. Negatively charged ions emerging from a desolvation capillary were guided by a radio frequency-only quadrupole ion-guide into an ion trap, where the ions were accumulated for 0.1 s before being pushed into the extraction zone of a time-of-flight mass spectrometer. The main anion signals corresponded to CuX_3^- and CuX_2^- as a result of redox reactions occurring during the electrospray.

In the PES experiment, the CuX_2^- anions of interest were mass-selected and decelerated before being intercepted by a laser beam in the detachment zone of the magnetic-bottle photoelectron analyzer. For the current study, 193 nm (6.424 eV) and 157 nm (7.866 eV) photons from an excimer laser were used for photodetachment. The photoelectrons were collected at nearly 100% efficiency by the magnetic-bottle and analyzed in a 4 m long time-of-flight tube. Photoelectron time-of-flight spectra were collected and then converted to kinetic energy spectra, calibrated by the known spectra of I^- and O^-. The binding energy spectra were obtained by subtracting the kinetic energy spectra from the corresponding photon energies. The energy resolution was about 10 meV (FWHM) at $\sim$0.5 eV kinetic energy, as measured from the spectrum of I^- at 355 nm.

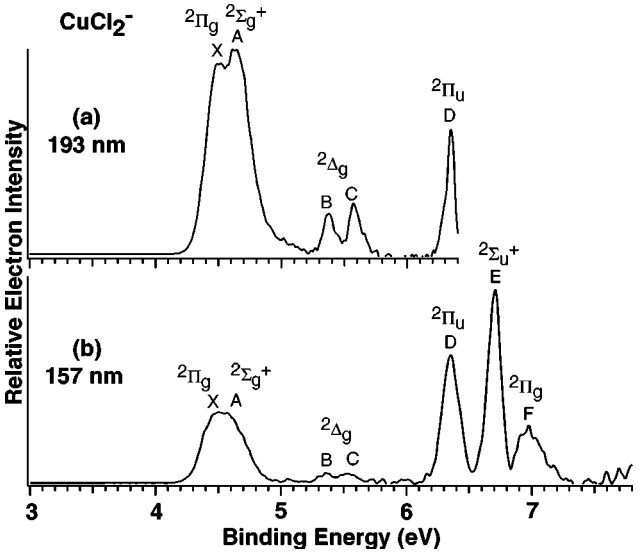

FIG. 1. Photoelectron spectra of $CuCl_2^-$, (a) at 193 nm (6.424 eV), (b) at 157 nm (7.866 eV).

III. COMPUTATIONAL DETAILS

The basis sets used were the aug-cc-pVTZ (Ref. 31) (with only one *f*-function of exponent 0.706) for Cl with the scalar relativistic (SR) Stuttgart pseudopotentials[32] for Cu and Br. For Br, the accompanying valence basis set was decontracted and augmented to give a (211111/21111/11/1) set (most diffuse functions, 0.045 for *s*, 0.072212 for *p*, 0.389 for *d*, and 0.706 for *f*). The basis set for bromine has been carefully fitted at the Hartree–Fock level and the electron affinity is not very sensitive to softer functions. We therefore neglected adding more diffuse functions for bromine. For Cu, the accompanying basis set was partially decontracted and augmented with further functions to give a (3111111/2211111/311111/111) set (most diffuse functions, 0.01 for *s*, *p*, and *d* and 0.4 for *f*).

Geometry optimizations and subsequent frequency analyses for the $^1\Sigma_g^+$ and $^2\Pi_g$ electronic ground states of CuX_2^- and CuX_2 ($X=Cl, Br$) were performed at the B3LYP and BPW91 level of theory using the GAUSSIAN98 program package.[33] Subsequent outer valence Green's function (OVGF) (Ref. 34) calculations at these geometries gave results not in very good agreement with the experimental data. We therefore performed CCSD(T) calculations using the unrestricted Hartree–Fock wave function as reference within the program package ACESII.[35] The CCSD(T) equilibrium geometries were determined by a numerical fit procedure. The frequency analyses for the $^2\Pi_g$ state of linear CuX_2 resulted in a symmetry-broken (nondegenerate) Π_u bending mode, due to the fact that a single determinant description is not sufficient and a state-averaged multireference procedure is

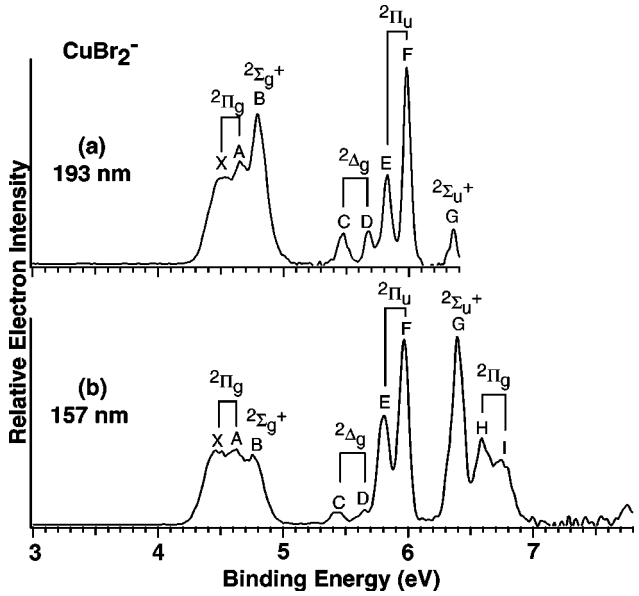

FIG. 2. Photoelectron spectra of $CuBr_2^-$, (a) at 193 nm (6.424 eV), (b) at 157 nm (7.866 eV).

required. We therefore report only the average frequency of the two modes, which has to be used with some care.

CCSD(T) optimizations for the neutral CuX_2 were only performed for the $^2\Pi_g$ ground state to yield the theoretical adiabatic EA. Otherwise single point CCSD(T) calculations at the CuX_2^- optimized CCSD(T) geometry were used to obtain the vertical electron detachment energies for the excited states of CuX_2. Spin–orbit coupling was neglected in all calculations. In order to correctly assign the spin–orbit states of $CuCl_2$ and $CuBr_2$ from Koopmans theorem we carried out fully relativistic Dirac–Hartree–Fock (DHF) calculations of the closed-shell anions using the program package DIRAC.[36] The all-electron basis sets used were of dual type and are described in Refs. 37 and 38.

IV. EXPERIMENTAL RESULTS

Figure 1 shows the PES spectra of $CuCl_2^-$ taken at 193 and 157 nm. The 193 nm spectrum exhibited five distinct features (X,$A-D$), in which the X and A bands were only partially resolved. At 157 nm, two more features (E and F) were revealed, while the X and A features could not be resolved due to the deteriorating instrumental resolution for the high kinetic energy electrons. The intensities of the B and C features at 193 nm [Fig. 1(a)] were relatively weak compared to that of the X, A, and D features, but were further reduced almost to the noise level at 157 nm [Fig. 1(b)]. The new feature F at 157 nm was also relatively weak.

The PES spectra of $CuBr_2^-$ (Fig. 2) were similar to that of $CuCl_2^-$, except that more features were observed apparently due to the larger spin–orbit splitting. There were in total ten distinct peaks (labeled from X, $A-I$) resolved at 157 nm. The H and I features and the high binding energy side of the G peak were cut off at 193 nm. The main differences between the 193 and 157 nm spectra were the intensity changes of the B, C, and D bands. The B peak was stronger in the 193 nm spectrum and became equal to the X and A bands at 157 nm. The C and D peaks, which were relatively weak at 193 nm, were further reduced at 157 nm, similar to the intensity changes of the B and C peaks in the $CuCl_2^-$ spectra.

TABLE I. Measured vertical detachment energies (VDE) for $CuCl_2^-$ and the obtained term values for $CuCl_2$ compared with spin–orbit averaged CCSD(T) calculations.

	Experiment			Calculated term value (cm^{-1})	
	State	VDE (eV)[a]	Term value (cm^{-1})[b]	This work	Ref. 9
X	$^2\Pi_g$	4.50(8)	0	0	0($^2\Pi_{g1/2}$) 178($^2\Pi_{g3/2}$)
A	$^2\Sigma_g^+$	4.63(8)	1050	859	1576
B	$^2\Delta_{g5/2}$	5.38(8)	7100	7768	7514
C	$^2\Delta_{g3/2}$	5.58(8)	8700		9656
D	$^2\Pi_u$	6.36(8)	15 000	16 410	16 686
E	$^2\Sigma_u^+$	6.71(8)	17 800	19 128	19 570
F	$^2\Pi_g$	6.97(10)	19 900		

[a]The numbers in the parentheses indicate the uncertainties in the last digits.
[b]Estimated using the VDE differences and rounded to 50 cm^{-1}.

The electron affinities (EAs) of CuX_2, or the adiabatic detachment energies (ADE) of the anions, are defined by the 0–0 transitions of the ground state features (the X bands). Due to the lack of vibrational resolution in the X bands, the EAs were determined approximately by drawing a straight line at the front edge of the X features and then adding a constant to the intercept with the binding energy axis, to take into account both the instrumental resolution and a finite thermal effect. Following this procedure, we found that the EAs of $CuCl_2$ and $CuBr_2$ were identical, 4.35 ± 0.05 eV within our experimental uncertainty. The vertical detachment energies (VDEs) were measured straightforwardly from the peak maxima and listed in Tables I and II for $CuCl_2^-$ and $CuBr_2^-$, respectively.

V. THEORETICAL RESULTS

Ground and excited electronic states of $CuCl_2$ and $CuBr_2$ have been investigated theoretically by a number of

TABLE II. Measured vertical detachment energies (VDE) for $CuBr_2^-$ and the obtained term values for $CuBr_2$ compared with spin–orbit averaged *ab initio* calculations.

	Experiment			CCSD(T)
	State	VDE (eV)[a]	Term value (cm^{-1})[b]	Term value (cm^{-1})
X	$^2\Pi_{g3/2}$	4.52(8)	0	0
A	$^2\Pi_{g1/2}$	4.65(8)	1050	
B	$^2\Sigma_g^+$	4.79(8)	2200	1609
C	$^2\Delta_{g5/2}$	5.47(8)	7650	7322
D	$^2\Delta_{g3/2}$	5.68(8)	9350	
E	$^2\Pi_{u3/2}$	5.83(8)	10 550	10 408
F	$^2\Pi_{u1/2}$	5.98(8)	11 800	
G	$^2\Sigma_u^+$	6.37(8)	14 900	13 360
H	$^2\Pi_{g3/2}$	6.59(8)	16 700	
I	$^2\Pi_{g1/2}$	6.74(10)	17 900	

[a]The numbers in the parentheses indicate the uncertainties in the last digits.
[b]Estimated using the VDE differences and rounded to 50 cm^{-1}.

TABLE III. Optimized bond lengths (in Å) for CuX_2^- and their neutrals at different levels of theory, and calculated, and experimental adiabatic and vertical detachment energies (ADE and VDE) at the scalar relativistic level. Experimental values are spin–orbit averaged.

Molecule	Property	B3LYP	BPW91	CCSD(T)	Expt. (this work)
$CuCl_2^-(D_{\infty h},{}^1\Pi_g)$	r_{CuCl} (Å)	2.140	2.124	2.116	
$CuCl_2(D_{\infty h},{}^2\Pi_g)$	r_{CuCl} (Å)	2.067	2.067	2.043	
	ADE (eV)	4.096	3.811	4.310	4.35±0.05
	VDE (eV)	4.190	3.861	4.316	4.50±0.08
$CuCl_2(D_{\infty h},{}^2\Sigma_g^+)$	r_{CuCl} (Å)	2.094	2.091	⋯	⋯
	ADE (eV)	4.412	4.456	⋯	⋯
	VDE (eV)	4.449	4.471	4.422	4.63±0.08
$CuCl_2(D_{\infty h},{}^2\Delta_g)$	r_{CuCl} (Å)	2.105	2.100	⋯	⋯
	ADE (eV)	5.286	5.692	⋯	⋯
	VDE (eV)	5.304	5.701	5.279	5.48±0.08
$CuBr_2^-(D_{\infty h},{}^1\Pi_g)$	r_{CuBr} (Å)	2.255	2.255	2.240	
$CuBr_2(D_{\infty h},{}^2\Pi_g)$	r_{CuBr} (Å)	2.200	2.200	2.167	
	ADE (eV)	4.084	3.759	4.309	4.4±0.05
	VDE (eV)	4.135	3.796	4.386	4.6±0.1
$CuBr_2(D_{\infty h},{}^2\Sigma_g^+)$	r_{CuBr} (Å)	2.233	2.231	⋯	
	ADE (eV)	4.576	4.581	⋯	
	VDE (eV)	4.583	4.589	4.416	4.79±0.08
$CuBr_2(D_{\infty h},{}^2\Delta_g)$	r_{CuBr} (Å)	2.239	2.234	⋯	
	ADE (eV)	5.352	5.730	⋯	
	VDE (eV)	5.355	5.753	5.270	5.57±0.08

authors.[8–11,39] Table III contains the equilibrium bond distances of CuX_2 and CuX_2^- and the electron detachment energies of CuX_2^-. Both the anions and neutral species were calculated to be linear. The structural data show the expected trends, with the bromide having longer bond lengths than the chloride. The structural differences between the anions and the neutrals are minor, approximately 0.07 Å for both the chloride and the bromide at the CCSD(T) level. All three methods appeared to reproduce the electron detachment energies of CuX_2^- reasonably well. The CCSD(T) values are in excellent agreement with the experimental results. In particular, the calculated ADEs for $CuCl_2^-$ and $CuBr_2^-$ at the CCSD(T) level of theory are nearly identical, consistent with the experimental observations. Further, the computations revealed that there was little difference between the ADEs and VDEs (~0.1 eV), consistent with the small geometry changes between the ground states of the anions and the neutrals. The calculated excitation energies (term values) for the excited states of CuX_2 at the CCSD(T) level (neglecting the spin–orbit coupling) are in good agreement with the experiments (Tables I and II), lending credence for the assignment for all the low-lying electronic states observed here.

Table IV lists an analysis of the seven highest occupied molecular orbitals (HOMOs) of CuX_2^- according to HF‖B3LYP calculations. For both relativistic methods (SRHF and DHF) and for both halides, the HOMO was found to be a π_g orbital in agreement with the fact that the ${}^2\Pi_g$ state represents the electronic ground state of CuX_2 (X=Cl and Br) (due to removal of an electron from the π_g HOMO of CuX_2^-). An examination of the MO coefficients indicates that this is an antibonding $sd_\pi(\mathrm{Cu})-p_\pi(\mathrm{X})$ orbital. A pictorial comparison of the four highest occupied molecular orbitals for $CuCl_2^-$ and $CuBr_2^-$ is given in Fig. 3.[40] An interesting feature in the comparison of some deeper orbitals (Fig. 4) is the presence of a small amount of $d_\pi-\pi^*$ bonding character for the chloride that does not occur for the bromide.

The orbital energies obtained from the DHF calculations reveal that for a specific spin–orbit split state the one with the larger ω value is highest in energy. This implies that removal of an electron gives $\mathrm{DE}(\Omega+1)<\mathrm{DE}(\Omega)$ for the detachment energies of a specific $\Lambda-S$ state in accordance with what one usually expects for hole states. We note that for $CuCl_2^-$ the $\sigma_g(1/2)$ and $\pi_g(1/2)$ orbitals are quasidegenerate and therefore mix due to spin–orbit coupling. The nonrelativistic single group notation for the $\Omega=1/2$ ${}^2\Pi_u$ and ${}^2\Sigma_g^+$ states of $CuCl_2$ may therefore be used with care.

The NBO (Ref. 41) and Mulliken charges for the negatively charged species are shown in Table V. A major difference between the two methods is that the NBO result shows less d_σ participation in the Cu–Cl bond. The B3LYP and BPW91 frequencies for the anion and neutral species are given in Table VI.

VI. SPECTRAL ASSIGNMENTS AND DISCUSSION

A. A brief overview of previous works

The absorption spectrum of $CuCl_2$ in the gas phase has been well known since the 1960s.[6,7] The first of these was by Hougen *et al.*[6] who assigned two broad features at ~9 000 and 18 000 cm^{-1} as two $d-d$ transitions, ${}^2\Pi_g\leftarrow{}^2\Sigma_g^+$, and ${}^2\Delta_g\leftarrow{}^2\Sigma_g^+$, respectively. The electronic spectrum was re-

TABLE IV. Occupied molecular orbitals of CuX_2^- at the scalar relativistic Hartree–Fock (SRHF) and Dirac–Hartree–Fock (DHF) level (calculated at the B3LYP geometry). A qualitative bonding description is also given.

$CuCl_2^-$		SRHF Koopmans energies (eV)	DHF Koopmans energies (eV)	Cu	X	Main character of MO
π_g	3/2	−6.069	−5.979	d_π	p_π	antibonding
	1/2		−6.119			
σ_g	1/2	−6.128	−6.051	sd_σ	p_σ	weakly antibonding
π_u	3/2	−6.876	−6.821		p_π	nonbonding
	1/2		−6.904			
σ_u	1/2	−7.247	−7.292		p_σ	nonbonding
δ_g	5/2	−8.790	−8.573	d_δ		nonbonding
	3/2		−8.844			
π_g	3/2	−9.553	−9.498	d_π	p_π	bonding, $d'-\pi^*$ bonding
	1/2		−9.515			
σ_g	1/2	−9.636	−9.742	sd_σ	p_σ	bonding
$CuBr_2^-$						
π_g	3/2	−5.641	−5.259	d_π	p_π	antibonding
	1/2		−5.590			
σ_g	1/2	−6.294	−6.100	sd_σ	p_σ	weakly antibonding
π_u	3/2	−6.234	−6.159		p_π	nonbonding
	1/2		−6.348			
σ_u	1/2	−6.618	−6.901		p_σ	nonbonding
δ_g	5/2	−9.118	−8.894	d_δ		nonbonding
	3/2		−9.166			
σ_g	1/2	−9.524	−9.844	sd_σ	p_σ	bonding
π_g	3/2	−9.629	−9.856	d_π		nonbonding
	1/2		−10.027			

corded at higher resolution later by DeKock and Gruen.[7] The same two-broad absorption systems at 8 700 and 19 000 cm^{-1} were observed. With simple ligand field calculations, they predicted two $d-d$ transitions $^2\Pi_g \leftarrow {}^2\Sigma_g^+$ at 3 800 cm^{-1} and $^2\Delta_g \leftarrow {}^2\Sigma_g^+$ at 8 200 cm^{-1}. Hence they assigned the 9 000 cm^{-1} band to the $^2\Delta_g \leftarrow {}^2\Sigma_g^+$ transition, but did not assign the observed 19 000 cm^{-1} band. They stated that the failure to observe the transition $^2\Pi_g \leftarrow {}^2\Sigma_g^+$ at 3 800 cm^{-1} was due to the instrumental limit (>4 000 cm^{-1}). De Mello *et al.*[8] performed the first *ab initio* SCF (RHF and UHF) studies

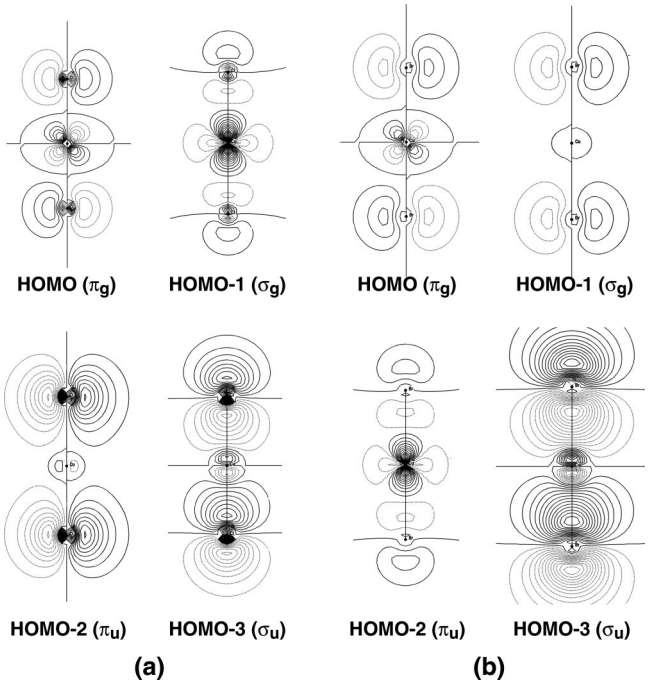

FIG. 3. Orbital plots of HOMO, HOMO-1, HOMO-2, and HOMO-3 of (a) $CuCl_2^-$ and (b) $CuBr_2^-$ (see also Table IV).

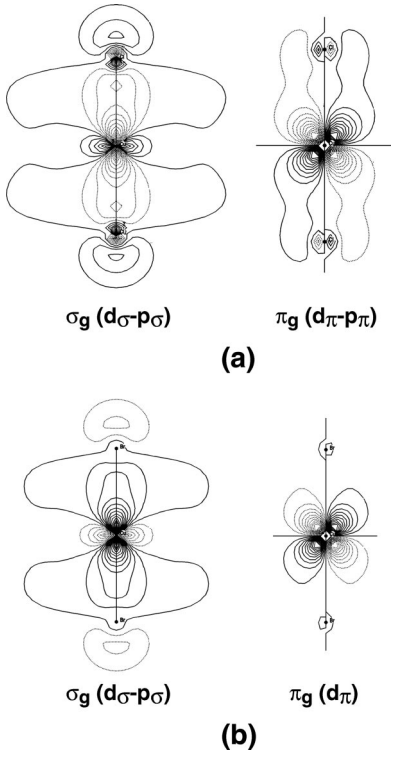

FIG. 4. σ_g bonding and π_g bonding/nonbonding molecular orbitals of (a) $CuCl_2^-$ and (b) $CuBr_2^-$.

TABLE V. Occupation of selected orbitals and partial charges (q) of CuX_2^-, based on NBO and Mulliken analyses of HF//B3LYP calculations.

			q_{NBO}	$q_{Mull.}$
Cu	$s^{0.44}$	$d^{9.79}$	0.654	0.035
Cl	$s^{1.95}$	$p^{5.79}$	−0.827	−0.517
Cu	$s^{0.37}$	$d^{9.93}$	0.673	0.381
Br	$s^{1.97}$	$p^{5.86}$	−0.836	−0.690

and multiple scattering $X\alpha$ calculations. They predicted at the SCF level that both the ligand field transitions from the ground state ($^2\Sigma_g^+$) to the $^2\Pi_g$ and $^2\Delta_g$ states were within the band at ~9 000 cm^{-1}, whereas the $^2\Pi_u$ and $^2\Sigma_u^+$ charge transfer states agreed with the band at 19 000 cm^{-1}. However, using multiple scattering X_α theory, they calculated that only the $^2\Pi_g$ state was at the IR region (6 198 cm^{-1}) and the $^2\Delta_g$ state lay at 23 961 cm^{-1}, even higher than the charge transfer state $^2\Pi_u$ (16 673 cm^{-1}). Bauschlicher and Roos (BR) (Ref. 9) later performed *ab initio* calculations, taking into account low-lying ligand field and charge transfer states and including single or double configuration interaction, coupled-pair functions, and spin–orbit interaction. They predicted that $CuCl_2$ has a ground state of $^2\Pi_{g(1/2)}$, contrary to all previous assignment of the ground state. They found that the $d-d$ transitions were: 178 cm^{-1} ($^2\Pi_{g(3/2)}$), 1 576 cm^{-1} ($^2\Sigma_g^+$), 7 514 cm^{-1} ($^2\Delta_{g(5/2)}$), and 9 656 cm^{-1} ($^2\Delta_{g(3/2)}$). The lowest charge transfer states were computed to lie at 16 686 cm^{-1} ($^2\Pi_u$) and 19 570 cm^{-1} ($^2\Sigma_u^+$). Therefore, they assigned the two bands at 9 000 and 19 000 cm^{-1} as the transitions of $^2\Delta_g \leftarrow {}^2\Pi_g(d-d)$ and $^2\Pi_u \leftarrow {}^2\Pi_g$, $^2\Sigma_u^+ \leftarrow {}^2\Pi_g$ (CT), respectively, which have since been used widely by experimentalists. Slightly later, Deeth[10] performed local density functional Slater-type orbital calculations. The $^2\Pi_g$ ground state for $CuCl_2$ was confirmed, and the two $d-d$ transitions of $^2\Sigma_g^+ \leftarrow {}^2\Pi_g$, $^2\Delta_g \leftarrow {}^2\Pi_g$ were predicted to be at 5 574 and 21 447 cm^{-1}, respectively, totally different from the calculations by BR. Nevertheless, Deeth was unable to assign the absorption transitions. The latest theoretical study of $CuCl_2$ was done by Rogemond *et al.*[11] using density functional theory with different exchange and correlation interactions. The ground state was confirmed to be $^2\Pi_g$. Among all different calculations performed by these authors, the energy levels for the three ligand field states (i.e., $^2\Pi_g$, $^2\Sigma_g^+$, $^2\Delta_g$) and the two charge transfer states (i.e., $^2\Pi_u$, $^2\Sigma_u^+$) were the same and were in the following sequence: $^2\Pi_g$, $^2\Sigma_g^+$, $^2\Pi_u$, $^2\Sigma_u^+$, $^2\Delta_g$, in order of increasing energies. Note, however, that this order differs from that predicted by the previous calculations of BR.[9] The energy levels for the low-lying states were predicted as 5 400 ($^2\Sigma_g^+$), 11 500 ($^2\Pi_u$), 17 300 ($^2\Sigma_u^+$), and 19 600 cm^{-1} ($^2\Delta_g$). Therefore, they proposed a new assignment for the two optical absorption bands with maxima at 9 000 and 19 000 cm^{-1} due to $^2\Sigma_g^+ \leftarrow {}^2\Pi_g(d-d)$, and $^2\Pi_u \leftarrow {}^2\Pi_g$ (CT), respectively.

TABLE VI. Vibrational frequencies of $CuCl_2^-$, $CuBr_2^-$, $CuCl_2$, and $CuBr_2$ (in cm^{-1}) in their electronic ground states.[a]

	Π_u	Σ_g^+	Σ_u^+
$CuCl_2^-$			
B3LYP	103	290	392
BPW91	104	297	399
$CuBr_2^-$			
B3LYP	78	187	323
BPW91	83	184	317
$CuCl_2$			
B3LYP	82	356	505
BPW91	91	345	485
Expt.	127,[b] 104[c]	370,[d] 360,[e] 372,[b] 358[c,f]	496,[d] 505[c]
$CuBr_2$			
B3LYP	86	188	341
BPW91	55	210	385

[a]Π_u, bending mode; Σ_g^+, symmetric stretch; Σ_u^+, asymmetric stretch.
[b]Reference 7(b).
[c]Reference 11.
[d]Reference 6(b).
[e]Reference 7(a).
[f]Reference 9.

B. Spectral assignments and discussion

Our calculated order of the MOs (Table IV) is similar to that obtained by Rogemond *et al.*,[11] except for the switch of the σ_u and δ_g MOs. Our results predict that the ground state of $CuCl_2^-$ has a valence configuration of $\sigma_g^2\pi_g^4\delta_g^4\sigma_u^2\pi_u^4\sigma_g^2\pi_g^4$. Upon removing one electron from the corresponding occupied MOs under the Koopmans' approximation, the final states of the $CuCl_2$ neutral molecule would be expected to be: $^2\Pi_g < {}^2\Sigma_g^+ < {}^2\Pi_u < {}^2\Sigma_u^+ < {}^2\Delta_g < {}^2\Pi_g < {}^2\Sigma_g^+$, respectively, in the order of increasing energy. Among these final states, the Π and Δ states are also expected to have spin–orbit splittings. However, our calculated results for the first five electronic states for $CuCl_2$ at the CCSD(T) level (without spin–orbit coupling) are as follows: $^2\Pi_g < {}^2\Sigma_g^+ < {}^2\Delta_g < {}^2\Pi_u < {}^2\Sigma_u^+$, as given in Table I. This ordering agrees with the results predicted by BR. The assignments of the PES spectra are according to these theoretical results, as shown in Fig. 1 and Table I. The *B* and *C* features are assigned to the spin–orbit components of the $^2\Delta_g$ state. Our observed spin–orbit splitting of 0.20 eV is very similar to the spin–orbit splitting of the ^2D state of the Cu atom (0.253 eV). The spin–orbit splitting for the $^2\Pi_g(X)$ ground state and the $^2\Pi_u(D)$ excited states is probably too small to be resolved. As we will see below, the spin–orbit splitting in the corresponding states of $CuBr_2$ is well resolved. There are two more highly excited state, $^2\Pi_g$ and $^2\Sigma_g^+$, corresponding to the removal of an electron from the deeper valence MOs, π_g and σ_g [Fig. 4(a)]. The vertical excitation energies could not be calculated at the CCSD(T) level of theory currently. The feature *F* at 6.97 eV [(Fig. 1(b))] should be due to one of these final states. The DHF calculations (Table IV) places the σ_g MO at a higher binding energy, which was likely the one not observed in our spectra. Thus we assign the *F* feature to the $^2\Pi_g$ state, as shown in Fig. 1(b). Again, as will be seen below, the spin–orbit splitting in the corresponding $^2\Pi_g$ state in $CuBr_2$ is well resolved. Overall, the excellent numeric agreement between the theoretical predictions and the PES

data for the excitation energies allow us to assign all the low-lying excited states observed here conclusively.

While the overall PES spectra of $CuBr_2^-$ are similar to that of $CuCl_2^-$, more features were observed due to the larger spin–orbit splitting as expected. Our DHF calculations (Table IV) yielded the following occupied valence MOs for $CuBr_2^-$: $\pi_g^4\sigma_g^4\delta_g^4\sigma_u^2\pi_u^4\sigma_g^2\pi_g^4$, which is almost identical to that for $CuCl_2^-$ except that the ordering of the two deeper π_g and σ_g MOs are different in the two systems (Table IV and Fig. 4). Detaching one electron from these MOs will result in the following final states for neutral $CuBr_2$: $^2\Pi_g$, $^2\Sigma_g^+$, $^2\Pi_u$, $^2\Sigma_u^+$, $^2\Delta_g$, $^2\Sigma_g^+$, and $^2\Pi_g$. Our CCST(T) results (Table II) predicted the same ordering of the first five low-lying states in $CuBr_2$ as in $CuCl_2$: $^2\Pi_g < ^2\Sigma_g^+ < ^2\Delta_g < ^2\Pi_u < ^2\Sigma_u^+$. The PES data for $CuBr_2^-$ are assigned accordingly, as shown in Table II and Fig. 2. The spin–orbit splitting and VDEs for the $^2\Delta_g$ state are nearly identical to those in $CuCl_2$, consistent with the fact that the δ_g MO is primarily of Cu $3d_\delta$ character. As expected, the spin–orbit splittings in the $^2\Pi_g$ (*X* and *A*) and $^2\Pi_u$ (*E* and *F*) states in $CuBr_2$ are much larger and well resolved (Fig. 2 and Table II). Similar to $CuCl_2$, we assigned the *H* and *I* features to the more highly excited $^2\Pi_g$ state. However, the DHF calculations here showed a significant discrepancy from the experimental observation regarding the character of the deeper π_g MO for $CuBr_2^-$ (Fig. 4). The expected increase of the spin–orbit splitting for the $^2\Pi_g$ state in $CuBr_2$ relative to that in $CuCl_2$ suggests that the deeper π_g MO is primarily of ligand character, whereas the DHF results predicted that this MO is mostly of Cu d_π character [(Fig. 4(b))]. Nevertheless, the similarity between the spectra of $CuBr_2^-$ and $CuCl_2^-$ lends significant support for the assignments of the $CuBr_2^-$ spectra.

A further comparison of the PES spectra of $CuCl_2^-$ and $CuBr_2^-$ (Figs. 1 and 2) is interesting. We note that the electron binding energies for the first three detachment channels, i.e., $^2\Pi_g$, $^2\Sigma_g^+$, and $^2\Delta_g$, are very similar in the two systems, suggesting their Cu $3d$ origin. On the other hand, the electron binding energies for the next three detachment channels, i.e., $^2\Pi_u$, $^2\Sigma_u^+$, and $^2\Pi_g$, are all decreased in the $CuBr_2^-$ spectra, relative to that in the $CuCl_2^-$ spectra. This observation is consistent with their ligand origins due to the relatively lower ionization potentials of Br. Such spectral changes among similar metal complexes with different ligands have been observed in several other systems and provide valuable information for spectral assignments, as well as for understanding the metal–ligand bonding.[26,28,42]

Based on the current results, we can definitely assign the famous IR and red bands observed in the optical absorption and emission of $CuCl_2$. The broad IR band with a maximum at 8 700 cm^{-1} is assigned to the $d-d$ transition, $^2\Delta_g \leftrightarrow ^2\Pi_g$ (7 100 and 8 700 cm^{-1}), whereas the red band with a maximum at ~19 000 cm^{-1}, is due to the CT transitions, $^2\Pi_u \leftrightarrow ^2\Pi_g$ (15 000 cm^{-1}) and $^2\Sigma_u^+ \leftrightarrow ^2\Pi_g$ (17 800 cm^{-1}). The $^2\Pi_g \leftarrow ^2\Pi_g$ (19 900 cm^{-1}) transition contributes to the red band absorption at the high energy side. The above assignment is consistent with the predictions of BR.

We have previously investigated alkali dihalides, MX_2^- (M=Li, Na;X=Cl, Br, I),[42] which would be isoelectronic with the CuX_2^- systems, except the Cu $3d$ shell. In addition, the alkali halides are all ionic systems, essentially consisting of M^+ and X^-. In the absence of any valence orbitals from the alkali centers, the PES spectral features of the alkali dihalides are due to removing electrons from the halide orbitals, resulting in extremely high electron binding energies (>5 eV for Cl and Br ligands).[42] The existence of the Cu $3d$ shell in CuX_2^- makes their electronic structures much richer and more interesting, resulting in the lower binding energy features in their PES spectra (Figs. 1 and 2), which do not exist in the alkali halide systems. It is these relatively low binding energy, Cu $3d$-derived valence states that give the redox properties of the CuX_2^- complexes. The first PES feature (X) in the CuX_2^- complexes (Figs. 1 and 2) correspond to a Cu(I)→Cu(II) oxidation reaction, albeit in the gas phase. As we have shown recently,[29] the shape of the detachment feature (the Franck–Condon envelope) in the gas phase contains valuable information concerning the energetics and reorganization energies of the Cu(I)/Cu(II) redox couple. The small difference between the ADE and VDE observed for CuX_2^- currently suggest a very small reorganization energies, as is also evident on the basis of the small geometry changes from the theoretical calculations (Table III).

VII. CONCLUSIONS

We report a combined PES and *ab initio* study of the two copper dihalide anions, $CuCl_2^-$ and $CuBr_2^-$. Distinct features observed in the PES spectra provide detailed electronic structure information on both the anion and neutral molecules. The electron affinities of $CuCl_2$ and $CuBr_2$ were measured to be identical, 4.35 ± 0.05 eV, which is in excellent agreement with the CCSD(T) calculations. The excitation energies of the low-lying excited states of the neutral molecules were determined experimentally for the first time. In conjunction with the results of the CCSD(T) calculations for the excited electronic states, the data allow a detailed and complete analysis and assignment of the low-lying states observed here, as well as a conclusive interpretation of two absorption bands observed previously for $CuCl_2$.

ACKNOWLEDGMENTS

The experimental work was supported by the National Science Foundation (CHE-9817811 to L.S.W.). Acknowledgment is also made to the Donors of the Petroleum Research Fund, administered by the American Chemical Society, for partial support of this research. The experiment was performed at the W. R. Wiley Environmental Molecular Sciences Laboratory, a national scientific user facility sponsored by Department of Energy's Office of Biological and Environmental Research and located at Pacific Northwest National Laboratory. Pacific Northwest National laboratory is operated for the U.S. Department of Energy by Battelle. L.S.W. is an Alfred P. Sloan Foundation Research Fellow. The Berlin group acknowledges support by the Volkswagenstiftung, the Deutsche Forschungsgemeinschaft (SFB 546), the Fonds der Chemsichen Industrie, and the Degussa-Hüls AG. The Konrad Zuse Zentrum is thanked for the generous allocation of computer time. The Auckland group acknowledges support from the Marsden fund (Wellington).

[1] (a) W. Kain and B. Schwederski, *Bioanorgansiche Chemie* (Teubner, Stuttgart, 1991); (b) F. A. Cotton, G. Wilkinson, C. A. Murillo, and M. Bochmann, *Advanced Inorganic Chemistry*, 6th ed. (Wiley, New York, 1999).
[2] E. I. Solomon and M. D. Lowery, Science **259**, 1575 (1993).
[3] R. H. Holm, P. Kennepohl, and E. I. Solomon, Chem. Rev. **96**, 2239 (1996).
[4] E. I. Solomon, U. M. Sundaram, and T. E. Machonkin, Chem. Rev. **96**, 2563 (1996).
[5] S. V. Didziulis, S. L. Cohen, A. A. Gewirth, and E. I. Solomon, J. Am. Chem. Soc. **110**, 250 (1988).
[6] (a) J. T. Hougen, G. E. Leroi, and T. C. James, J. Chem. Phys. **34**, 1670 (1961); (b) G. E. Leroi, T. C. James, J. T. Hougen, and W. Klemperer, *ibid.* **36**, 2879 (1962).
[7] (a) C. W. DeKock and D. M. Gruen, J. Chem. Phys. **44**, 4387 (1966); (b) F. Dienstbach, F. P. Emmenegger, and C. W. Schlapher, Helv. Chim. Acta **60**, 2460 (1977).
[8] P. C. de Mello, M. Hehenberger, S. Larsson, and M. Zerner, J. Am. Chem. Soc. **102**, 1278 (1980).
[9] C. W. Bauschlicher, Jr. and B. O. Roos, J. Chem. Phys. **91**, 4785 (1989).
[10] R. J. Deeth, J. Chem. Soc. Dalton Trans. **1993**, 1061 ().
[11] F. Rogemond, H. Chermette, and D. R. Salahub, Chem. Phys. Lett. **219**, 228 (1994).
[12] P. Schwerdtfeger, P. D. W. Boyd, G. A. Bowmaker, and L. P. Aldridge, Struct. Chem. **1**, 405 (1990).
[13] (a) M. P. Barnes, R. T. Carter, N. M. Lakin, and J. M. Brown, J. Chem. Soc., Faraday Trans. **89**, 3205 (1993); (b) A. J. Ross, P. Crozet, R. Bacis, S. Churassy, B. Erba, S. H. Ashworth, N. M. Lakin, M. R. Wickham, I. R. Beattie, and J. M. Brown, J. Mol. Spectrosc. **177**, 134 (1996).
[14] P. Crozet, J. C. Coste, R. Bacis, A. J. Bouvier, S. Churassy, and A. J. Ross, Chem. Phys. **178**, 505 (1993).
[15] A. J. Bouvier, E. Bosch, and A. Bouvier, Chem. Phys. **202**, 139 (1996).
[16] P. Crozet, A. J. Ross, R. Bacis, M. P. Barnes, and J. M. Brown, J. Mol. Spectrosc. **172**, 43 (1995).
[17] A. J. Ross, R. Bacis, A. J. Bouvier, S. Churassy, J. C. Coste, P. Crozet, and I. Russier, J. Mol. Spectrosc. **158**, 27 (1993).
[18] S. Yoshida, M. Taniwaki, T. Sawano, K. Shimizu, and T. Fujioka, Jpn. J. Appl. Phys. **28**, L831 (1989).
[19] S. Yoshida, K. Shimizu, T. Sawano, T. Tokuda, and T. Fujioka, Appl. Phys. Lett. **54**, 2400 (1989).
[20] T. Tokuda, N. Fujii, S. Yoshida, K. Shimizu, and I. Tanaka, Chem. Phys. Lett. **174**, 385 (1990).
[21] A. J. Bouvier, R. Bacis, J. Bonnet, S. Churassy, P. Crozet, B. Erba, J. B. Koffend, J. Lamarre, M. Lamrini, D. Pigache, and A. J. Ross, Chem. Phys. Lett. **184**, 133 (1991).
[22] H. P. Yang, Y. Qin, T. J. Cui, Q. N. Yuan, X. B. Xie, Q. Zhuang, and C. H. Zhang, Chem. Phys. **191**, 130 (1992).
[23] T. Tokuda and N. Fujii, J. Phys. Chem. **96**, 6504 (1992).
[24] R. Huang, R. Zhang, and R. N. Zare, Chem. Phys. Lett. **170**, 437 (1990).
[25] L. S. Wang, C. F. Ding, X. B. Wang, and S. E. Barlow, Rev. Sci. Instrum. **70**, 1957 (1999).
[26] X. B. Wang and L. S. Wang, J. Chem. Phys. **111**, 4497 (1999).
[27] X. B. Wang and L. S. Wang, J. Am. Chem. Soc. **122**, 2096 (2000).
[28] X. B. Wang and L. S. Wang, J. Am. Chem. Soc. **122**, 2339 (2000).
[29] X. B. Wang and L. S. Wang, J. Chem. Phys. **112**, 6959 (2000).
[30] X. B. Wang and L. S. Wang, J. Phys. Chem. A **104**, 4429 (2000).
[31] D. E. Woon and T. H. Dunning, Jr., J. Chem. Phys. **98**, 1358 (1993).
[32] M. Dolg, U. Wedig, H. Stoll, and H. Preuss, J. Chem. Phys. **86**, 866 (1987).
[33] GAUSSIAN 98, Revision A.7, M. J. Frisch, G. W. Trucks, H. B. Schlegel *et al.* (Gaussian, Inc., Pittsburgh, PA, 1998).
[34] J. V. Ortiz, V. G. Zakrzewski, and O. Dolgounircheva, in *Conceptual Perspectives in Quantum Chemistry*, edited by J.-L. Calais and E. Kryachko (Kluwer, Academic, 1997), p. 465.
[35] J. F. Stanton, J. Gauss, J. D. Watts *et al.*, ACESII (University of Florida, Gainesville, 1995).
[36] T. Saue, T. Enveldson, T. Helgaker, H. J. A. Jensen, J. K. Laerdahl, K. Ruud, J. Thyssen, and L. Visscher, program DIRAC, A relativistic *ab initio* Electronic Structure Program (Odense, Denmark, 1998).
[37] P. Pernpointner, M. Seth, and P. Schwerdtfeger, J. Chem. Phys. **108**, 6722 (1998).
[38] J. K. Laerdahl and P. Schwerdtfeger, Phys. Rev. A **60**, 4439 (2000).
[39] (a) T.-K. Ha and M. T. Nguyen, Z. Naturforsch. Teil A **39**, 175 (1984); (b) G. A. Bowmaker, P. D. W. Boyd, and R. J. Sorrenson, J. Chem. Soc., Faraday Trans. **81**, 1627 (1985); (c) M.-M. Rohmer, A. Grand, and M. Benard, J. Am. Chem. Soc. **112**, 2875 (1990).
[40] Schaftenaar, G. *MOLDEN 3.2*, CAOS/CAMM Center, The Netherlands, 1996.
[41] A. E. Reed, L. A. Curtiss, and F. Weinhold, Chem. Rev. **88**, 899 (1988).
[42] X. B. Wang, C. F. Ding, L. S. Wang, A. I. Boldyrev, and J. Simons, J. Chem. Phys. **110**, 4763 (1999).